J Fluoresc (2014) 24:153–160
DOI 10.1007/s10895-013-1281-z

ORIGINAL PAPER

Synthesis and Optical Properties of Various Thienyl Derivatives of Pyrene

Krzysztof R. Idzik · Tobias Licha · Vladimír Lukeš · Peter Rapta · Jaroslaw Frydel · Mario Schaffer · Eric Taeuscher · Rainer Beckert · Lothar Dunsch

Received: 16 May 2013 / Accepted: 18 July 2013 / Published online: 6 August 2013

Abstract A series of various thienyl derivatives of pyrene were synthesized by Stille cross-coupling procedure. Their structures were characterized by ^{1}H NMR, ^{13}C NMR and elemental analysis. The spectroscopic characteristics were investigated by UV–vis absorption and fluorescence spectra. Based on quantum chemical calculations, the energy levels of investigated molecules with respect to the pyrene molecule were also discussed.

Keywords Stille cross-coupling procedure · Absorption · UV–VIS · Fluorescence spectroscopy · Pyrene · Thiophene

K. R. Idzik · E. Taeuscher · R. Beckert
Institute of Organic and Macromolecular Chemistry, Friedrich-Schiller University Jena, Humboldstraße 10, 07743 Jena, Germany

K. R. Idzik (✉) · T. Licha (✉) · M. Schaffer
Department Applied Geology, Geoscience Centre of the University of Göttingen, Goldschmidtstr. 3, 37077 Göttingen, Germany
e-mail: krzysztof.idzik@pwr.wroc.pl
e-mail: tobias.licha@geo.uni-goettingen.de

V. Lukeš · P. Rapta
Institute of Physical Chemistry and Chemical Physics, Slovak University of Technology Bratislava, Radlinského 9, SK-812 37 Bratislava, Slovak Republic

P. Rapta · L. Dunsch
Group of Electrochemistry and Conducting Polymers, Leibniz-Institute for Solid State and Materials Research, 01171 Dresden, Germany

J. Frydel
VENITUR Sp. z o.o., ul Wawozowa 34 B, 31-752 Krakow, Poland

Introduction

Organic compounds containing extended π-conjugation have received immense attention in recent years due to their unique photophysical and charge transport properties, which make them good material for potential applications in electronic devices such as organic light emitting diodes (OLEDs) [1–5], organic photovoltaics (OPV) [6–10] organic thin film transistors (OTFT) [11–13], etc. They are also attractive due to their promising two photon absorption [14, 15] and nonlinear optical [16, 17] characteristics. Among the π-conjugated molecular materials, those containing polyaromatic hydrocarbons (PAH), such as anthracene [18–20] perylene [21], pyrene [22–24], pentacene [25, 26], etc., tethered with each other by vinyl or acetylene linkages, are especially attractive due to their flat π-stacking organization in the solid state. Direct C−C linkage between the PAH has been found to be detrimental to the extension of conjugation as there is a loss of coplanarity owing to the steric congestion [27].

The most attractive π-center within two-photon materials is a pyrene moiety, not only because it is planar but also because it has been extensively studied in various fields of chemical biology. Moreover, due to durable electronic properties of the pyrene moeiety, its derivatives have found applications in microenvironmental sensors [28–30], liquid crystals [31, 32], organic light-emitting diodes [33], photoactive polypeptides [34], and genetic probes [35–37], and serve as components for various types of fluorescent polymers and dendrimers [38–40].

The pyrene core is particularly interesting in this context since it offers numerous possibilities of peripheral group modifications with profound consequences on the condensed-matter structure. For example, non-substituted pyrene forms monoclinic crystals, while tetraethynylpyrene derivatives of

phenylethynyl form liquid crystalline columnar phases [41], and pyrenes similarly substituted with n-diethyleneglycolether derivatives display a liquid phase at room temperature [42]. Perylene is a typical luminescence material which has been investigated for several decades. However, selfquenching will appear at high concentrations or pure crystals due to molecular aggregation [43]. On the other side, the luminescence properties of pyrene core might be modulated using the proper molecular substitution, e.g. with the heterocyclic units. For example, the linear oligo- or polythiophenes have both an excellent performance when acting as a building material of organic solar cells [44] and high hole mobility in organic field effect transistors [45]. Thiophene derivatives of pyrenes generally display promising optical and electrochemical properties. Organic π-conjugated structures containing thiophene units undergo both oxidation and reduction processes and play an important role in the search for new materials and their novel applications [44]. Oligothiophenes with well defined structures have also received a great deal of attention not only as an example of model compounds for conducting polythiophenes, but also as a new class of functional π-electron systems.

To gain deeper insight into the relations between the structure and optical properties of the thienyl-pyrene derivatives, we will present the comparative spectroscopic and theoretical study of six novel molecular materials based on a pyrene core that is connected to thiophene units at the 1, 3, 6, and 8 positions: 1-(2-thienyl)-pyrene, 1,6-bis(2-thienyl)-pyrene, 1,4-bis(2-thienyl)-pyrene, 1,3,6-tris(2-thienyl)-pyrene and 1,3,6,8-tetra(2-thienyl)-pyrene. In this context, the origin of the vibronic structure of pyrene and 1,3,6,8-tetra(2-thienyl)-pyrene fluorescence spectra will be analyzed using a simple model based on the Franck-Condon analysis.

Methods and Materials

Preparation

All chemicals, reagents, and solvents were used as purchased from commercial sources without further purification. ^{1}H NMR and ^{13}C NMR spectra were recorded in $CDCl_3$ on 300, 500 and 600 MHz liquid state Bruker spectrometer. Chemical shifts are denoted in δ unit (ppm) and referenced to the internal standard: TMS (tetramethylsilane) at 0.0 ppm. The splitting patterns are annotated as follows: s (singlet), d (doublet), t (triplet) and m (multiplet). Preparative column chromatography was carried out on glass columns of different sizes packed with silica gel: Merck 60 (0.035–0.070 mm). Melting points of the synthesized dyes were determined using a Stuart smp 20 melting point apparatus.

The chemical structure and synthetic route of the pyrene derivatives are illustrated in Scheme 1. Bromination of pyrene (**1**) with one to four equivalents of bromine gave the mono-, di-, tri-, and tetrabromopyrenes: 1-bromopyrene (**2**), 1,6-dibromopyrene (**3**), 1,4-dibromopyrene (**4**), 1,3,6-tribromopyrene (**5**), and 1,3,6,8-tetrabromopyrene (**6**) [45].

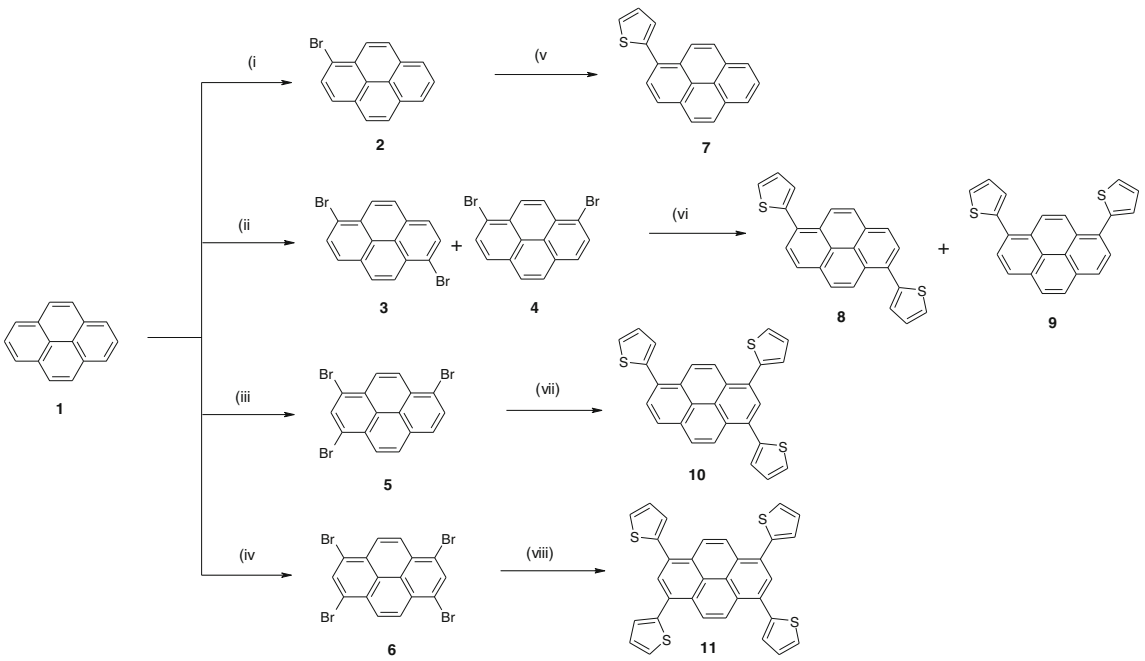

Scheme 1 Synthesis of pyrene derivatives, (i): Br_2, DCM, (ii): 2 eq Br_2, DCM, (iii): 3 eq Br_2, nitrotoluene, (iv): 4 eq Br_2, nitrotoluene, (v): 2-(tributylstannyl)thiophene, $Pd(PPh_3)_4$, toluene, (vi): 2 eq 2-(tributylstannyl) thiophene, $Pd(PPh_3)_4$, toluene, (vii): 3 eq 2-(tributylstannyl)thiophene, $Pd(PPh_3)_4$, toluene, (viii): 4 eq 2-(tributylstannyl)thiophene, $Pd(PPh_3)_4$, toluene

Mono- and dibromopyrene were prepared in DCM, in case of tri- and tetrabromopyrene we used nitrotoluene as a solvent. Cross-coupling of these bromopyrenes with 2-(tributylstannyl)thiophene under the conditions of the Stille reaction afforded mono-, bis-, tris-, and tetra(thienyl)pyrenes **7**–**11**. 2-(tributylstannyl)thiophene (**2** – 2.0 mmol, **5** – 6.0 mmol, **6** – 8 mmol, **3** and **4** – 4 mmol) respectively and $Pd(PPh_3)_4$ (0.46 g, 0.4 mmol) were added under nitrogen to compound **2** or **5** or **6** or a mixture of non separated **3** and **4** (2.0 mmol) dissolved in 150 mL of anhydrous toluene in a 250 mL round two-bottom flask. The resulting mixture was stirred for 4 days at 110 °C. Subsequently, the mixture was cooled down to room temperature. Water (100 mL) was added and the resulting solution was extracted three times with 50 mL of $CHCl_3$. The combined organic layers were washed with 50 mL brine, dried over $MgSO_4$ and evaporated until brown oil appeared. The crude product (**7**–**11**) was purified by column chromatography (hexane/AcOEt, 10:1). For preparation of bis(thienyl)pyrenes we used a mixture of 1,6-dibromopyrene (**3**) and 1,4-dibromopyrene (**4**). We successfully isolated 1,6-bis(thienyl)pyrene (**8**) from 1,4-bis(thienyl)pyrene (**9**). These latter derivatives were purified through a chromatography column. The structures of compounds **7**–**11** were confirmed by NMR and elemental analysis. The reactions were conducted under easy-to-perform, mild conditions with moderate to good yields. Finally, the chemical substitution leads to an increase of the melting points (m.p.) what ensures the thermal stability of these materials.

1-(2-thienyl)-pyrene (**7**) colorless crystals, 95 % yield, m.p. 85–86 °C. ^{1}H NMR (600 MHz, $CDCl_3$): δ=8.48 (d, J=9.6 Hz, 1H); 8.18 (d, J=7.8 Hz, 1H); 8.17 (d, J=7.8 Hz, 2H); 8.09–8.05 (m, 4H); 8.01 (t, J=7.5 Hz, 1H); 7.51 (dd, J=5.4, 1.2 Hz, 1H); 7.37 (dd, J=3.6, 1.2 Hz, 1H); 7.25 (dd, J=5.1, 3.3 Hz, 1H). ^{13}C NMR (500 MHz, $CDCl_3$): δ=142.5; 131.4; 130.9; 130.8; 129.7; 129.0; 128.4; 127.9; 127.8; 127.7; 127.4; 127.2; 126.1; 126.0; 125.2; 125.0; 124.9; 124.7; 124.5. Elemental analysis for: $C_{20}H_{12}S$ Calc.: C, 84.47; H, 4.25; S, 11.27. Found: C, 84.72; H, 4.33; S, 11.31.

1,6-Bis(2-thienyl)-pyrene (**8**) Yellow solid, 80 % yield, m.p. 238–239 °C. ^{1}H NMR (600 MHz, $CDCl_3$): δ=8.49 (d, J=9.0 Hz, 2H); 8.17 (d, J=7.8 Hz, 2H); 8.09 (d, J=7.8 Hz, 2H); 8.07 (d, J=9.6 Hz, 2H); 7.51 (d, J=4.8 Hz, 2H); 7.37 (d, J=3.6 Hz, 2H) 7.04 (dd, J=4.8, 3.6 Hz, 2H). ^{13}C NMR (500 MHz, $CDCl_3$): δ=142.5; 130.8; 130.1; 129.5; 128.8; 128.0; 127.8; 127.5; 126.3; 125.4; 125.1; 124.6. Elemental analysis for: $C_{24}H_{14}S_2$ Calc.: C, 78.65; H, 3.85; S, 11.50. Found: C, 78.45; H, 3.92; S, 11.37.

1,4-Bis(2-thienyl)-pyrene (**9**) Yellow solid, 10 % yield, m.p. 129–130 °C. ^{1}H NMR(600 MHz, $CDCl_3$): δ=8.50 (s, 2H); 8.18 (d, J=7.8 Hz, 2H); 8.10 (d, J=7.8 Hz, 2H); 8.08 (s, 2H); 7.51 (d, J=5.4 Hz, 2H); 7.37 (d, J=3.6 Hz, 2H); 7.25 (dd, J=4.8, 1.8 Hz, 2H). ^{13}C NMR (500 MHz, $CDCl_3$): δ=142.4; 131.2; 129.8; 128.8; 128.6; 128.0; 127.6; 127.5; 126.2; 125.5; 125.1; 124.9. Elemental analysis for: $C_{24}H_{14}S_2$ Calc.: C, 78.65; H, 3.85; S, 11.50. Found: C, 78.79; H, 3.73; S, 11.76.

1,3,6-Tris(2-thienyl)-pyrene (**10**) Yellow solid, 90 % yield, m.p. 154–155 °C. ^{1}H NMR (600 MHz, $CDCl_3$): δ=8.53–8.45 (m, 3H); 8.12 (s, 1H); 8.16 (d, J=7.8 Hz, 1H); 8.10 (d, J=7.8 Hz, 1H); 8.07 (d, J=9.6 Hz, 1H); 7.52–7.49 (m, 3H); 7.39–7.36 (m, 3H); 7.26–7.22 (m, 3H). ^{13}C NMR (500 MHz, $CDCl_3$): δ=142.4; 142.0; 141.9; 131.1; 131.0; 130.2; 129.8; 129.5; 129.4; 129.3; 128.9; 128.8; 128.3; 128.2; 128.1; 127.5; 126.4; 126.3; 126.1; 125.8; 125.7; 125.5; 125.3; 124.9. Elemental analysis for: $C_{28}H_{16}S_3$ Calc.: C, 74.96; H, 3.59; S, 21.44. Found: C, 75.29; H, 3.67; S, 21.46.

1,3,6,8-Tetra(2-thienyl)-pyrene (**11**) Yellow solid, 80 % yield, m.p. 291–292 °C. ^{1}H NMR (300 MHz, $CDCl_3$): δ=8.52 (s, 4H); 8.24 (s, 2H); 7.53 (d, J=4.8 Hz, 4H); 7.41 (d, J=3.3 Hz, 4H); 7.28–7.24 (m, 4H). ^{13}C NMR (500 MHz, $CDCl_3$): δ=141.9; 131.2; 129.8; 129.1; 128.4; 127.5; 126.5; 125.9; 125.8. Elemental analysis for: $C_{32}H_{18}S_4$ Calc.: C, 72.42; H, 3.42; S, 24.16. Found: C, 72.58; H, 3.63; S, 24.19.

Optical Measurements

The UV/VIS absorbance spectra were recorded on a Cary 50 spectrophotometer (Varian) between 250 and 500 nm at a scanning rate of 60 nm/min. Fluorescence spectra were recorded on a Cary Eclipse spectrofluorometer (Agilent) equipped with a xenon lamp excitation source. The excitation was set at the maximum of the lowest excitation band in the range 2.76–3.18 eV (450 to 390 nm). The scanning rate was 30 nm min^{-1} with a slit width for excitation and emission of 2.5 nm, respectively. The measurements were carried out at 20±0.1 °C in Peltier-thermostatted quartz cells (Hellma Analytics, Müllheim) having a path length of 1.0 cm.

Quantum-Chemical Methods

The electronic ground (S_0) and lowest (S_1) state geometries of the selected molecules were optimized at the Density Functional Theory (DFT) [46] level of theory employing Becke's three parameter hybrid functional using the Lee, Yang and Parr correlation functional (B3LYP) [47]. The vertical transition energies, oscillator strengths and corresponding gradients between the initial and final states were computed by the Time Dependent (TD)-DFT method [48]. The calculations of optimal geometries were performed using the 6-31G(d) basis set for C, H atoms and 6-31+G(d) basis set for S atom [49, 50] (the energy cut-off of 5×10^{-4} hartree and the final root mean square energy gradient below 4×10^{-4} hartree $Å^{-1}$). These calculations were done using Northwest Computational Chemistry Package (NWChem) 6.1.1 program package [51]. Based on these calculations, the origin of vibronic structure in experimental fluorescence spectrum of pyrene and largest thienyl-pyrene derivate (**11**) was explained using the Franck-

Table 1 The experimental absorption (λ_{abs}), fluorescence excitation (λ_{exc}) and fluorescence emission (λ_{em}) spectral characteristics for compounds **1**, 7, **8**, **9**, **10** and **11**. TD-B3LYP ΔE energies for the $S_0 \rightarrow S_1$ and $S_1 \rightarrow S_0$ transitions

Compound	λabs /nm	ΔE(S0 → S1) eV (nm)	λexc /nm	λem /nm	ΔE(S1 → S0) eV (nm)
pyrene (1)	333a)	3.72 (333)		373 a)	3.45 (359)
1-(2-thienyl)-pyrene (7)	347	3.38 (366)	399	425	2.97 (417)
1,6-Bis(2-thienyl)-pyrene (8)	371	3.14 (395)	412	437	2.70 (459)
1,4-Bis(2-thienyl)-pyrene (9)	370	3.14 (395)	411	438	2.77 (448)
1,3,6-Tris(2-thienyl)-pyrene (10)	388	2.97 (418)	437	461	2.66 (466)
1,3,6,8-Tetra(2-thienyl)-pyrene (11)	404	2.82 (440)	443	471	2.43 (510)

a) measured in methanol [53]

Condon analysis based on the Poisson distribution and harmonic approximation [52, 53].

Results and Discussion

The basic pyrene molecule is planar and it contains four fused rings of D_{2h} symmetry group. The B3LYP geometry optimisation of the smallest molecule with one added thienyl ring (**7**) showed that the mutual orientation of the thiophene moiety with respect to the pyrene plane for the most stable conformation is Θ=48°. The thiophene ring is spatially oriented out of the pyrene center. With respect to this fact, this arrangement was also fixed for the next monomers. In the case of the molecules **8**, **9** and **11**, the geometries were symmetric and they belong to the C_2 and C_{2h} point of groups, respectively. Based on the optimal DFT electronic ground state geometries, the vertical excitation energies were calculated. The energies corresponding to the lowest $S_0 \rightarrow S_1$ tranistions have very strong oscillator strengths and they are collected in Table 1. The highest energy value is indicated for pyrene molecule 3.72 eV and the symmetry of this electronically allowed tranistions is 1^1B_{2u}. The consecutive addition of the lateral thiophenes, leads to the red shift with the energies of 3.38 eV (for **7**) to 2.82 eV (for **11**). The symmetry of the electronic transition for the largest molecule **11** is 1^1A_u. The next relative high oscillator strengths are connected with the energies 4.65 eV for **1** ($S_0 \rightarrow S_5$), 4.30 eV for **7** ($S_0 \rightarrow S_4$), 4.21 eV for **8** ($S_0 \rightarrow S_5$), 3.92 eV for **9** ($S_0 \rightarrow S_3$), 3.78 eV for **10** ($S_0 \rightarrow S_4$) and 3.68 eV for **11** ($S_0 \rightarrow S_4$).

These theoretical energies agree very well with the the spectroscopic properties measured in chloroform solution. As it is illustrated in Fig. 1, the absorption spectra of the studied systems are formed from two main bands. The maxima of the lowest energy absorption bands for **7** to **11** are located between 347 nm and 404 nm, depending on the molecular structure and molecular size. The obtained characteristic properties of the absorption maxima (λ_{abs}) are collected in Table 1. The maximum of the second absorption bands are also changed with respect to the molecular size. The

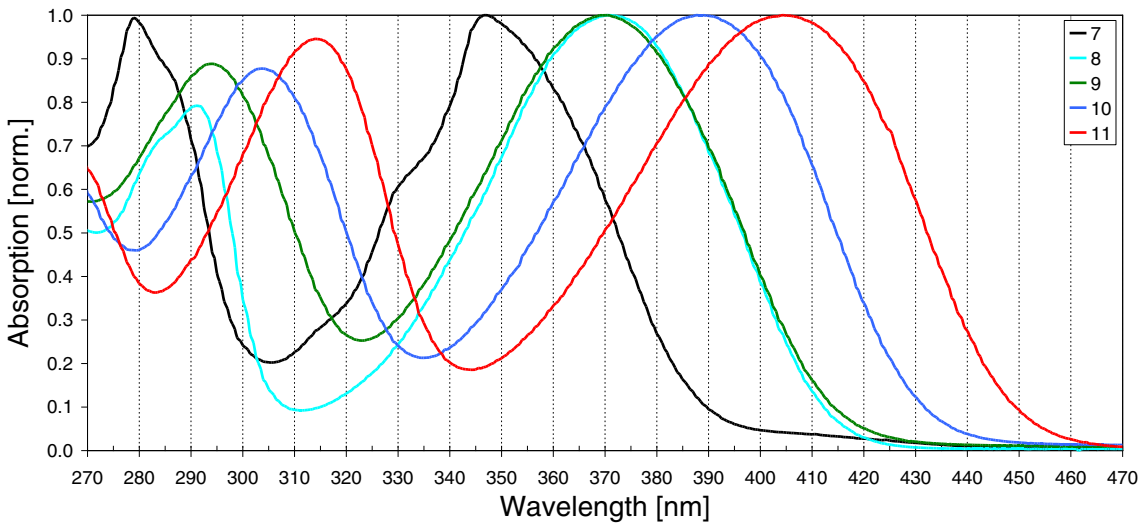

Fig. 1 Normalized UV/VIS-absorption spectra of **7**, **8**, **9**, **10**, and **11** solvated in $CHCl_3$

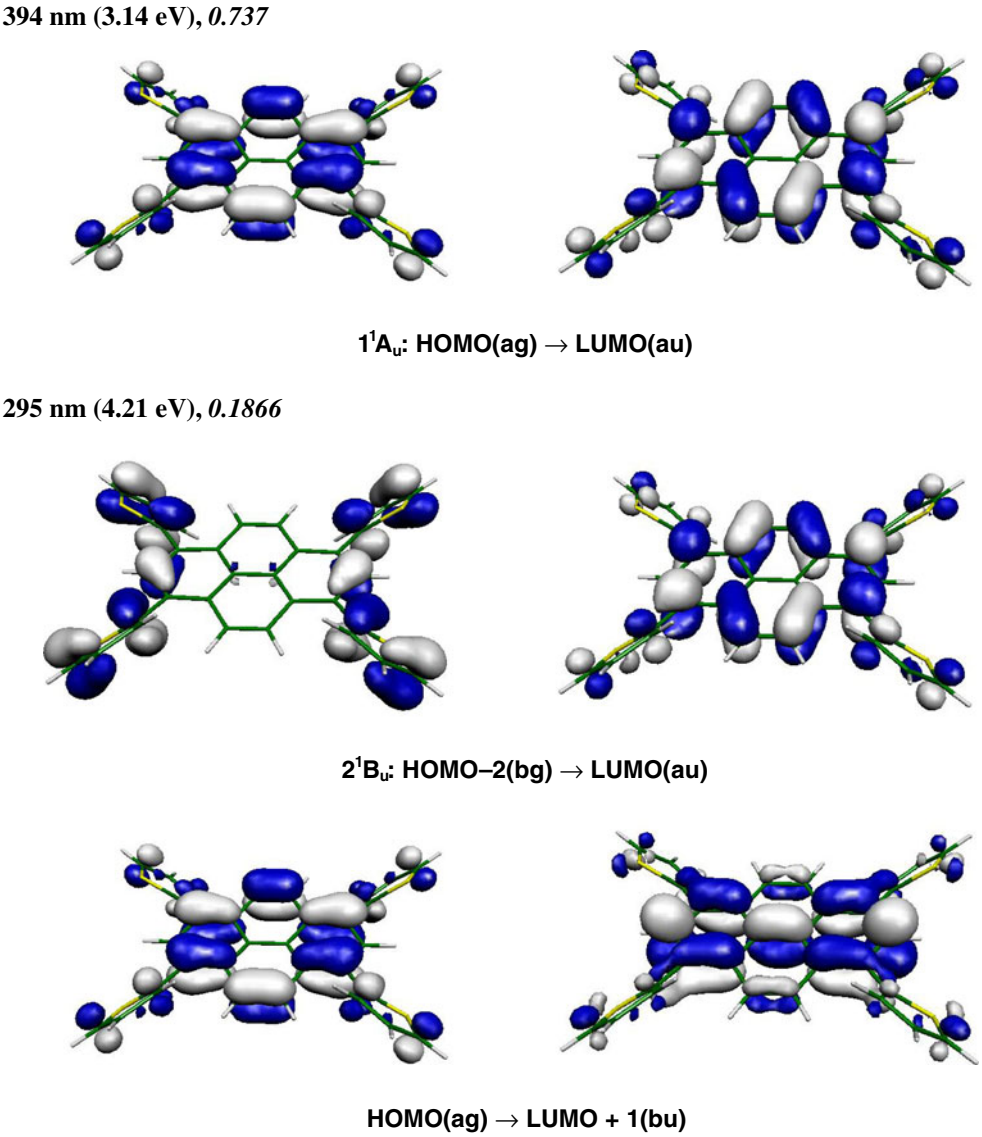

Fig. 2 B3LYP orbitals of contributing dominantly to the lowest TD-B3LYP energy tranistions ($S_0 \rightarrow S_1$ and $S_0 \rightarrow S_4$). The depicted isosurface is 0.03 atomic unit. The values written in italic are oscillator strengths. Orbital symmetry is indicated in the parentheses

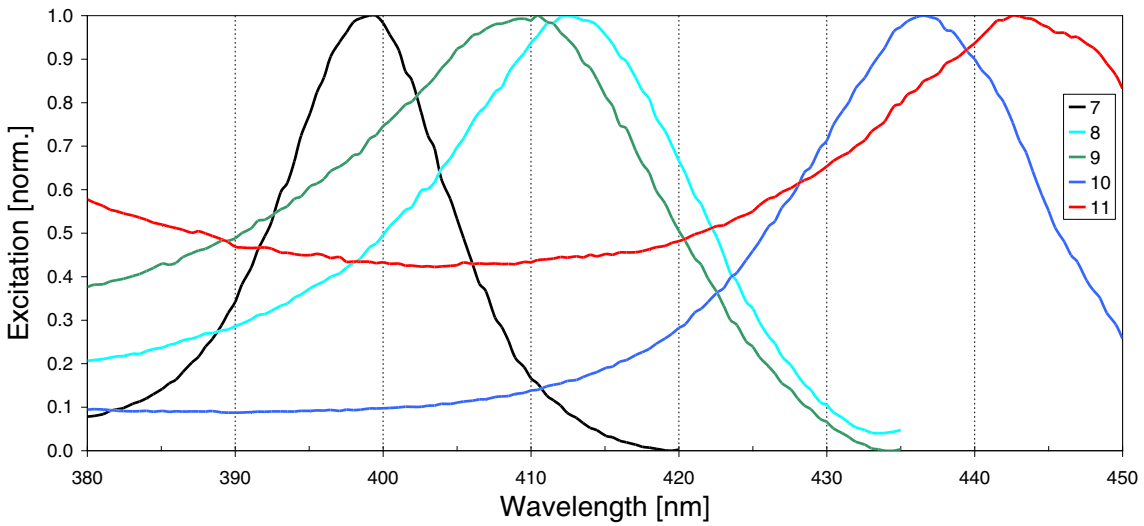

Fig. 3 Normalized fluorescence excitation spectra of **7**, **8**, **9**, **10**, and **11** solvated in $CHCl_3$

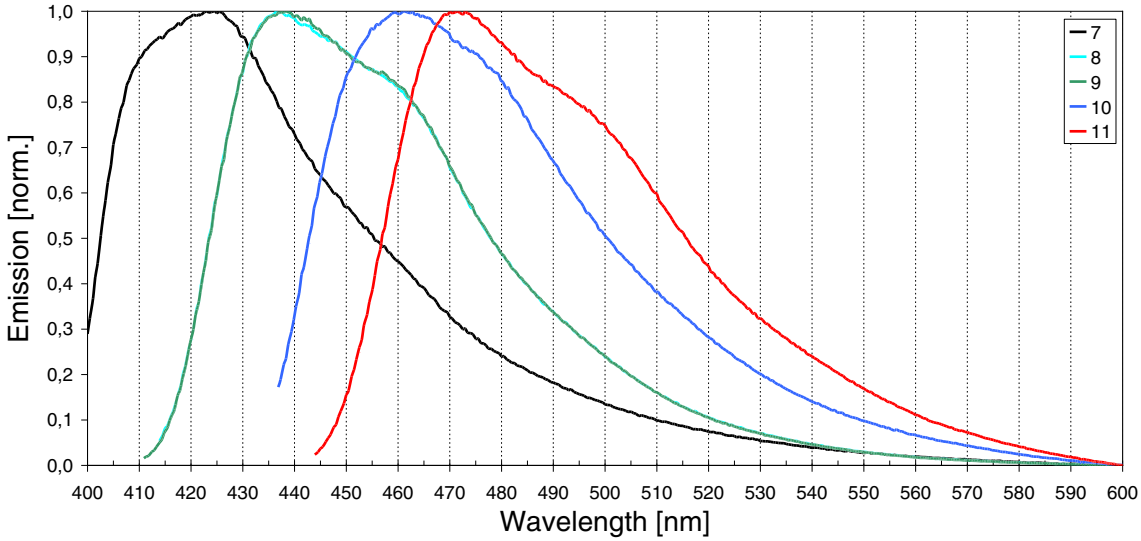

Fig. 4 Normalized fluorescence emission spectra of **7**, **8**, **9**, **10**, and **11** solvated in $CHCl_3$

corresponding wavelengths reported by Lukeš et al. [53] for the pyrene molecule in methanol are 333 and 270 nm. Pyrene with one thienyl group gives an absorption maximum at 347 nm, with two groups at approximately 370 nm, with three—at 388, and with four—at 404 nm. Thus, an increasing number of thienyl groups in the pyrene ring results in a bathochromic shift.

In order to understand the effect of the molecular structure on the absorption spectra of the largest molecule **11** for the two lowest optical transitions with dominant oscillator strength, it is useful to examine the relevant highest occupied (HOMO) and lowest unoccupied (LUMO) molecular orbitals. These orbitals were evaluated for B3LYP functional (see Fig. 2). Our calculations showed that the electron transition $S_0 \rightarrow S_1$ fo 1^1A_u symmetry is mostly connected with the excitation from HOMO to LUMO. The HOMO orbital is regularly delocalized over the outer carbon–carbon bonds of pyrene and thiophene moities. On the other hand, the lobes of LUMO orbital are perpendicularly oriented to the lobes of HOMO. The next intensive optically allowed transition of 2^1B_u symmetry comes from HOMO–2 to LUMO and HOMO to LUMO+1 orbitals. As it is illustrated in Fig. 2, this electronic excitation shifts the electron denisty from the lateral thiophene units to the pyrene center.

From the structural point of view, the electron excitation is also responsible for the planarization of all monomers ($\Theta \approx 36°$). The next geometrical changes are also indicated along the C–C and C–S bonds. The energies belonging to the $S_1 \rightarrow S_0$ de-excitations have also very strong oscillator strengths and they are collected in Table 1. These values are also dependent on the number of thiophene units and they agree with the corresponding experimental trends.

The fluorescence excitation and steady-state emission spectra of the thienylpyrenes were recorded also in chloroform (Figs. 3 and 4). In all cases, the comparable fluorescence activity was observed. The substitution of hydrogens in the pyrene ring by thiophene groups result in a bathochromic shift. The fluorescence excitation maxima (λ_{exc}) for compounds **7**–**11** are shifted from 399 to 443 nm (see Table 1). Similar effect is also perceivable in the experimental fluorescence emission band maxima (λ_{em}). An increasing number of thienyl groups connected to pyrene causes a displacement of the spectral band positions in the fluorescence emission spectra from 425 to 471 nm (Fig. 4). The corresponding fluorescence wavelength reported by Lukeš et al. [53] for the pyrene molecule in methanol is 373 nm.

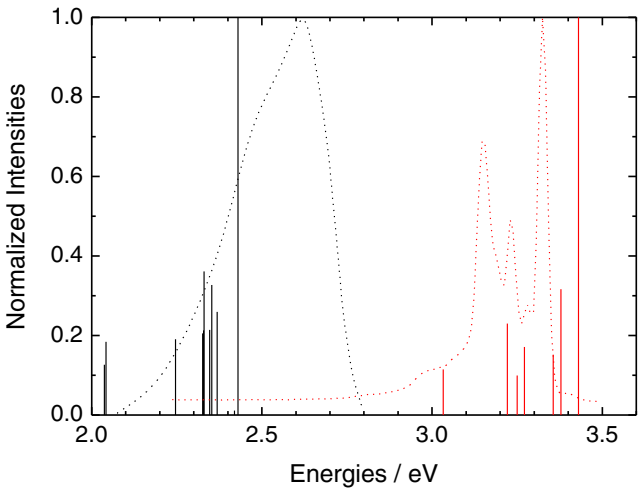

Fig. 5 Calculated TD-B3LYP fluorescence $S_1 \rightarrow S_0$ vertical transition with the vibrational replicas (see the *solid lines*) for the pyrene (**1**) and 1,3,6,8-tetra(2-thienyl)-pyrene (**11**). Normalized fluorescence spectrum of pyrene molecule was measured in methanol [53]

To estimate the influence of the thienyl addition to the pyrene moiety on the vibronic progression for de-excitation $S_1 \rightarrow S_0$, the relevant Huang-Rhys factors were calculated from the (TD)-B3LYP geometries and normal modes for the molecules **1** and **11**. The quantum mechanical B3LYP calculations of the molecular normal modes reveal that the observed spectral structure for pyrene is dominated by a composite progression of the modes at 412, 597, 1277, 1450, 1686 and 3205 cm^{-1} with HR factors higher than 0.2. In the case of the largest molecule **11**, the theoretically determined modes are at 85, 508, 831, 849, 859, 1529 and 3231 cm^{-1}. All these vibrations belong to the A_g symmetry and they correspond to the C −C aromatic ring deformations, CH out-of-plane vibrations, out-of-plane CH and CCC bending and C–H stretching vibrations (see Ref. 29 for pyrene modes). Based on the obtained TD-B3LYP HR factors for **1** and **11**, the relative intensities of the replica were calculated for relevant normal modes and these vertical lines were visualized with respect to the TD-B3LYP de-excitation energy with the relative intensity being equal 1. The depicted theoretical data (see solid lines in Fig. 5) show that the presence of thienyl groups is evidently responsible for the broadening of fluorescence emission band comparing to the pyrene emission spectrum. These findings well correspond with the experimental fluorescence records.

Conclusions

In this work we have presented the synthesis and combined theoretical and photophysical characteristics of the new molecular materials based on a pyrene core which was connected to thiophene units. Following Stille cross-coupling procedure, we obtained various thienyl derivatives of pyrene in good yield and purity. Based on the theoretical and experimental results, we can conclude that the optical properties of the whole synthesized series depend evidently on the number of thienyl rings present on the pyrene molecule. A typical red shift effect was observed when the monosubstituted derivative displayed violet emission, while the tetrathienyl pyrene exhibited blue emission. The theoretical calculations for **11** also showed that seven vibrations of A_g symmetry serve as coupling modes to the allowed electronic transition from the lowest to ground states. It is plausible to expect that the integration of thiophene and pyrene in a molecular structure seem to be potentially good starting-point materials for industrial applications with respect to the thermal stability and optical properties.

Acknowledgments This work was realized within the European Union Project (SNIB, MTKD-CT-2005-029554). This support is gratefully acknowledged. The presented study was partially funded by the German Federal Ministry of Environment (promotional reference No. 0325417, Reaktherm).

For the financial support Peter Rapta and Vladimír Lukeš thank the Scientific Grant Agency of the Slovak Republic (Projects No. VEGA 1/1072/11, 1/0735/13, 1/0289/12).

References

1. Sun Y, Giebink NC, Kanno H, Ma B, Thompson ME, Forrest SR (2006) Nature 440:908–912
2. Hancock JM, Gifford AP, Zhu Y, Lou Y, Jenekhe SA (2006) Chem Mater 18:4924–4932
3. Lyu YY, Kwak J, Kwon O, Lee SH, Kim D, Lee C, Char K (2008) Adv Mater 20:2720–2729
4. Tonzola CJ, Kulkarni AP, Gifford AP, Kaminsky W, Jenekhe SA (2007) Adv Funct Mater 17:863–874
5. Duan L, Hou L, Lee TW, Qiao J, Zhang D, Dong G, Wang L, Qiu YJ (2010) J Mater Chem 20:6392–6407
6. Zhan X, Tan ZA, Domercq B, An Z, Zhang X, Barlow S, Li Y, Zhu D, Kippelen B, Marder SR (2007) J Am Chem Soc 129:7246–7247
7. Ning Z, Tian H (2009) Chem. Commun 5483–5495.
8. Hagfeldt A, Boschloo G, Sun L, Kloo L, Pettersson H (2010) Chem Rev 110:6595–6663
9. Clifford JN, Martínez-Ferrero E, Viterisi A, Palomares E (2011) Chem Soc Rev 40:1635–1646
10. Zhan XW, Facchetti A, Barlow S, Marks TJ, Ratner MA, Wasielewski MR, Marder SR (2011) Adv Mater 23:268–284
11. Sundar VC, Zaumseil J, Podzorov V, Menard E, Willett RL, Someya T, Gershenson ME, Rogers JA (2004) Science 303:1644–1647
12. Jung BJ, Tremblay NJ, Yeh M-L, Katz HE (2011) Chem Mater 23:568–582
13. Niimi K, Shinamura S, Osaka I, Miyazaki E, Takimiya K (2011) J Am Chem Soc 133:8732–8739
14. Sumalekshmy S, Henary MM, Siegel N, Lawson PV, Wu YG, Schmidt K, Bredas J-L, Perry JW, Fahrni CJ (2007) J Am Chem Soc 129:11888–11889
15. He GS, Tan L-S, Zheng Q, Prasad PN (2008) Chem Rev 108:1245–1330
16. Terenziani F, Painelli A, Katan C, Charlot M, Blanchard-Desce M (2006) J Am Chem Soc 128:15742–15755
17. Nakano M, Kishi R, Yoneda K, Inoue Y, Inui T, Shigeta Y, Kubo T, Champagne B (2011) J Phys Chem A 115:8767–8777
18. Wee KR, Han WS, Kim JE, Kim AL, Kwon S, Kang SO (2011) J Mater Chem 21:1115–1123
19. Zhu MR, Wang QA, Gu Y, Cao XS, Zhong C, Ma DG, Qin JG, Yang CL (2011) J Mater Chem 21:6409–6415
20. Cho I, Kim SH, Kim JH, Park S, Park SY (2012) J Mater Chem 22:123–129
21. Wurthner F, Stolte M (2011) Chem Commun 47:5109–5115
22. Shimizu H, Fujimoto K, Furusyo M, Maeda H, Nanai Y, Mizuno K, Inouye M (2007) J Org Chem 72:1530–1533
23. Xia RD, Lai WY, Levermore PA, Huang W, Bradley DDC (2009) Adv Funct Mater 19:2844–2850
24. Figueira-Duarte TM, Müllen K (2011) Chem Rev 111:7260–7314
25. Li S, Jia ZY, Nakajima K, Kanno K, Takahashi T (2011) J Org Chem 76:9983–9987
26. Qu HM, Cui WB, Li JL, Shao JJ, Chi CY (2011) Org Lett 13:924–927
27. Kozma E, Munno F, Kotowski D, Bertini F, Luzzati S, Catellani M (2010) Synth Met 160:996–1001
28. Pu L (2004) Chem Rev 104:1687
29. Martinez-Manez R, Sancenon F (2003) Chem Rev 103:4419
30. Yuasa H, Miyagawa N, Izumi T, Nakatani M, Izumi M, Hashimoto H (2004) Org Lett 6:1489
31. Hassheider Y, Benning SA, Kitzerow HS, Achard MF, Bock H (2001) Angew Chem Int Ed 40:2060
32. De Halleux V, Calbert JP, Brocorens P, Cornil J, Declercq JP, Brédas JL (2004) Geerts Y AdV Funct Mater 14:649
33. Daub J, Engl R, Kurzawa J, Miller SE, Schneider S, Stockmann A, Wasielewski MR (2001) J Phys Chem A 105:5655
34. Jones G, Vullev VI (2002) Org Lett 4:4001
35. Saito Y, Miyauchi Y, Okamoto A, Saito I (2004) Chem Commun 1704
36. Hwang GT, Seo YJ, Kim BH (2004) J Am Chem Soc 126:6528

37. Yamana K, Fukunaga Y, Ohtani Y, Sato S, Nakamura M, Kim W J, Akaide T, Maruyama A (2005) Chem Commun 2509
38. Baker LA, Crooks RM (2000) Macromolecules 33:9034
39. Modrakowski C, Flores SC, Beeinhoff M, Schluter AD (2001) Synthesis 2143
40. Hayer A, de Halleux V, Kohler A, El-Garoughy A, Meijer EW, Barbera J, Tant J, Levin J, Lehmann M, Gierschner J, Cornil J, Geerts YH (2006) J Phys Chem B 110:7653
41. Hayer A, de Halleux V, Kohler A, El-Garoughy A, Meijer E, Barbera J, Tant J, Levin J, Lehmann M, Gierschner J, Cornil J, Geerts YJ (2006) Phys Chem B 110:7653
42. de Halleux V, Mamdouh W, De Feyter S, De Schryver F, Levin J, Geerts Y (2006) J Photochem Photobiol, A 178:251
43. Mi BX, Gao ZQ, Lee CS, Lee ST, Kwong HL, Wong NB (1999) Appl Phys Lett 75:4055–4057
44. Mishra A, Ma CQ, Bäuerle P (2009) Chem Rev 109:1141
45. Ogino K, Iwashima S, Inokuchi H (1965) HaradaY Bull Chem Soc Jpn 38:473–477
46. Barone V (1996) Recent advances in density functional methods, Part I. World Scientific Publishing, Singapore
47. Becke A (1993) Density-functional thermochemistry. 3. The role of exact exchange. J Chem Phys 98:5648–5652
48. Furche F, Ahlrichs R (2002) Adiabatic time-dependent density functional methods for excited state properties. J Chem Phys 117:7433–7447
49. Petersson G, Al-Laham M (1991) A complete basis set model chemistry. 2. Open-shell systems and the total energies of the 1st-row atom. J Chem Phys 94:6081–6090
50. Rassolov V, Ratner M, Pople J, Redfern P, Curtiss L (2001) 6-31G* basis set for third-row atoms. J Comput Chem 22:976–984
51. Valiev M, Bylaska EJ, Govind N, Kowalski K, Straatsma TP, van Dam HJJ, Wang D, Nieplocha J, Apra E, Windus TL, de Jong WA (2010) Comput Phys Commun 181:1477
52. Siebrand W (1967) J Chem Phys 46:440
53. Lukeš V, Ilčin M, Kollár J, Hrdlovič P, Chmela S (2010) Chem Phys 377(1–5):123–131